

ALTERNATING HEEGAARD DIAGRAMS AND WILLIAMS SOLENOID ATTRACTORS IN 3-MANIFOLDS

CHAO WANG — YIMU ZHANG

ABSTRACT. We find all Heegaard diagrams with the property “alternating” or “weakly alternating” on a genus two orientable closed surface. Using these diagrams we give infinitely many genus two 3-manifolds, each admits an automorphism whose non-wandering set consists of two Williams solenoids, one attractor and one repeller. These manifolds contain half of Prism manifolds, Poincaré’s homology 3-sphere and many other Seifert manifolds, all integer Dehn surgeries on the figure eight knot, also many connected sums. The result shows that many kinds of 3-manifolds admit a kind of “translation” with certain stability.

1. Introduction

In [7], Smale introduced the solenoid attractor into dynamics as an example of indecomposable hyperbolic non-wandering set. It has a nice geometric model, namely the nested intersections of solid tori. Suppose f is a fibre preserving embedding from a disk fibre bundle N over S^1 into itself, contracting the fibres

2010 *Mathematics Subject Classification*. Primary: 57N10, 37C70, 37D45; Secondary: 57M12.

Key words and phrases. Heegaard diagram; solenoid attractor; Prism manifold; Poincaré’s homology 3-sphere; figure eight knot.

The authors would like to thank Professor Shicheng Wang and Xiaoming Du for their many helpful discussions.

The authors were partially supported by the National Natural Science Foundation of China (Grant No. 11371034).

and inducing an expansion on S^1 , then $\bigcap_{i=1}^{\infty} f^i(N)$ is a so-called Smale solenoid. To generalize this kind of construction, in [9], Williams introduced solenoid attractors derived from expansions on 1-dimensional branched manifolds. It also has a geometric model, as the nested intersections of handlebodies.

For a 3-manifold M , many of these attractors can be realized by the geometric models with suitable automorphisms $f \in \text{Diff}(M)$. But in most cases the realization will not be global. Global means that the non-wandering set $\Omega(f)$ is the union of solenoid attractors and repellers. Here a repeller of f is an attractor of f^{-1} . By standard arguments in dynamics, one can show that if $\Omega(f)$ consists of solenoid attractors and repellers, then there must be exactly one attractor and one repeller, and f is like a “translation” on M .

Motivated by the study in Morse theory and Smale’s work in dynamics, the following question was suggested in [3] by Jiang, Ni and Wang who studied this global realization question for Smale solenoids.

QUESTION. When does a 3-manifold admit an automorphism whose non-wandering set consists of solenoid attractors and repellers?

In [3], they showed that for a closed orientable 3-manifold M , there is a diffeomorphism $f: M \rightarrow M$ with the non-wandering set $\Omega(f)$ a union of finitely many Smale solenoids IF and ONLY IF M is a Lens space $L(p, q)$ with $p \neq 0$, namely M has Heegaard genus one and is not $S^1 \times S^2$. They also showed that the diffeomorphism f constructed in the IF part is Ω -stable, but is not structurally stable.

In the opinion of [3], a manifold M admitting a dynamics f such that $\Omega(f)$ consists of one hyperbolic attractor and one hyperbolic repeller presents a symmetry of the manifold with certain stability. The simplest example is the sphere, which admits a dynamics f such that $\Omega(f)$ consists of exactly two hyperbolic fixed points, a sink and a source. Lens spaces give us more such examples when we consider more complicated attractors. It is believed by Jiang, Ni and Wang that many more 3-manifolds admit such symmetries if we replace the Smale solenoids by the Williams solenoids. As a special case, Wang asked whether the Poincaré’s homology 3-sphere admits such a symmetry. What about hyperbolic 3-manifolds?

Similar with the discussion in [3], in [5], Ma and Yu showed that for a closed orientable 3-manifold M , if there is $f \in \text{Diff}(M)$ such that $\Omega(f)$ consists of Williams solenoids, whose defining handlebodies have genus $g \leq 2$, then the Heegaard genus $g(M) \leq 2$. On the other hand, to construct such M and f , they introduced the alternating Heegaard splitting which is a genus two splitting and admits a so-called alternating Heegaard diagram (see Definition 2.5). They showed that if M admits an alternating Heegaard splitting, then there is f such

that $\Omega(f)$ consists of two Williams solenoids, whose defining handlebodies have genus two. As an interesting example, they showed that the truncated-cube space (see [4]), whose fundamental group is the extended triangle group of order 48, admits an alternating Heegaard splitting.

The motivation of this paper is to find further such examples. As special cases, we will show that the Poincaré’s homology 3-sphere and many hyperbolic 3-manifolds admit such “symmetries with certain stability”. Hence we give a partial answer to the questions asked by Wang.

Concretely, let $S^2(a, b, c)$ denote the Seifert fibred spaces with base S^2 and three singular fibres having invariants a, b, c . For example, $S^2(-1/2, 1/4, 1/3)$ is the truncated-cube space. Let $P(m, n)$ denote the manifolds $S^2(-1/2, 1/2, m/n)$, which are the so-called Prism manifolds, the simplest 3-manifolds other than Lens spaces.

THEOREM 1.1. *Every 3-manifold M in the following classes admits an alternating Heegaard splitting:*

- $P(m, n)$, $0 < m < n$, $(m, n) = 1$.
- $S^2(-1/2, 1/4, m/n)$, $0 < m < n/2$, $(m, n) = 1$.
- $L(n, m) \# S^1 \times S^2$, $L(n, m) \# RP^3$, $0 \leq m < n$, $(m, n) = 1$.

Also there are infinitely many hyperbolic 3-manifolds admitting such splittings. For these 3-manifolds there exists $f \in \text{Diff}(M)$ such that $\Omega(f)$ consists of two Williams solenoids.

In fact, we can find all alternating Heegaard diagrams on a genus two orientable surface. They can be determined by integral vectors (n, k_1, k_2, k_3) , which satisfy $n > 0$ and the greatest common divisor $(n, k_1 + k_2 + 2k_3) = 1$. The 3-manifolds in Theorem 1.1 come from special diagrams.

On the other hand, having an alternating Heegaard splitting is a strong restriction to genus two 3-manifolds. As it is pointed out in [5], if M admits an alternating Heegaard splitting, then $H_1(M, \mathbb{Z}_2) \neq 0$. Hence we cannot apply the result in [5] to the Poincaré’s homology 3-sphere. After a modification, we generalize the alternating Heegaard splitting to the weakly alternating Heegaard splitting (see Definition 5.1), which also guarantees the existence of the required f .

THEOREM 1.2. *If a closed orientable 3-manifold M admits a weakly alternating Heegaard splitting, then there is a diffeomorphism $f \in \text{Diff}(M)$ such that $\Omega(f)$ consists of two Williams solenoids.*

We can also find all so-called weakly alternating Heegaard diagrams and for a part of them we can identify the corresponding 3-manifolds. Notice that the Poincaré’s homology 3-sphere has the form $S^2(-1/2, 1/3, 1/5)$. For all $l \in \mathbb{Z}$, let $S_{l/1}^3(4_1)$ denote the $l/1$ -surgery on the figure eight knot.

THEOREM 1.3. *Every 3-manifold M in the following classes admits a weakly alternating Heegaard splitting:*

- $S_{l/1}^3(4_1)$.
- $S^2(-1/2, 1/l, m/n)$, $0 < m < n$, $(m, n) = 1$.
- $S^2(1/l, 1/r, 1/n)$, $n > 0$.
- $L(n, m) \# L(l, 1)$, $0 \leq m < n$, $(m, n) = 1$.

For these 3-manifolds there exists $f \in \text{Diff}(M)$ such that $\Omega(f)$ consists of two Williams solenoids.

Here l and r can be any integer. In the second and third classes if l or r is 0, then we will get connected sums rather than Seifert fibred spaces. Notice that in each class there are infinitely many 3-manifolds with $H_1(M, \mathbb{Z}_2) = 0$.

By the same argument as in [3], one can show that all f we constructed are Ω -stable, but not structurally stable. Theorems 1.1 and 1.3 convince us that there are many more 3-manifolds admitting such “symmetries with certain stability”. Surely all (weakly) alternating Heegaard diagrams can give us many kinds of manifolds in the Thurston’s picture of 3-manifolds. But at present we can only recognize a part of them.

In Section 2, we give some basic definitions, including the handcuffs solenoid, alternating Heegaard diagram and alternating Heegaard splitting. Then we give a brief introduction to the construction of the required $f \in \text{Diff}(M)$, appearing in [3] and [5]. Then we divide the proof of Theorem 1.1 into two steps: In Section 3, we will find all alternating Heegaard diagrams. In Section 4, we identify for special alternating Heegaard diagrams what 3-manifolds they give, hence give a proof of Theorem 1.1.

The discussion of weakly alternating Heegaard splitting (diagram) will be parallel to the alternating case. In Section 5, we introduce weakly alternating Heegaard splitting (diagram) and give a proof of Theorem 1.2. Then we will find all weakly alternating Heegaard diagrams. In Section 6, we identify for special weakly alternating Heegaard diagrams what 3-manifolds they give, hence give a proof of Theorem 1.3. At the end of the paper we give some further remarks.

2. Basic definitions and constructions

2.1. Handcuffs solenoid and alternating Heegaard diagram. All Williams solenoids we consider will have the following geometric model. For general definition and more details one can see [9].

Let N be a genus two handlebody with the C^r ($r \geq 1$) “disk fibre bundle” structure, fibred over the branched C^r manifold K , as in Figure 1. Let p denote the projection map $N \rightarrow K$. We always suppose there is a Riemannian metric on N .

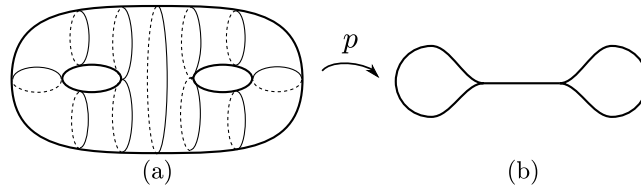


FIGURE 1. Disk bundle and handcuffs.

Suppose $f: N \rightarrow N$ is a fibre preserving C^r map such that $f: N \mapsto f(N)$ is a diffeomorphism, and the induced map $g: K \rightarrow K$ is an immersion. We also require:

Contracting condition on fibres: for each fibre D , $f(D)$ lies in the interior of a fibre and $\lim_{i \rightarrow \infty} \text{Diameter}(f^i(D)) = 0$.

Expanding condition on K : g is an expansion and $\Omega(g) = K$. Moreover, each point of K has a neighbourhood whose image under g is an arc.

Here “the immersion g is an expansion” means that there is a Riemannian metric $\|\cdot\|$ on the tangent bundle $T(K)$ and constants $C > 0, \lambda > 1$, such that

$$\|(Dg)^n(v)\| \geq C\lambda^n\|v\|, \quad \text{for all } n \in \mathbb{Z}^+, v \in T(K).$$

REMARK 2.1. The expanding condition can be required for self immersions of general branched manifolds. In our case K is like handcuffs. Any open set of K will be mapped onto K by g^n for large n . Then g is an expansion implies $\Omega(g) = K$.

Figure 2 is an example of such f and the corresponding immersion g .

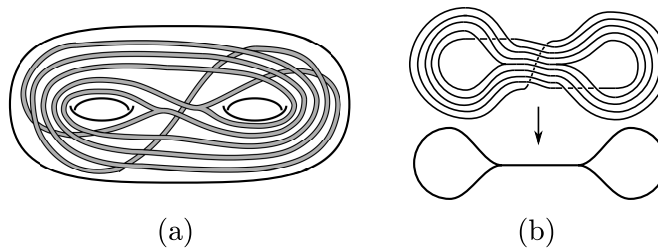


FIGURE 2. Embedding and expansion.

DEFINITION 2.2. We call $\Lambda_f = \bigcap_{i=1}^{\infty} f^i(N)$ a handcuffs solenoid with a defining neighbourhood N and a “shift map” $f|_{\Lambda_f}$.

REMARK 2.3. Let Σ be the inverse limit of the sequence $K \leftarrow K \leftarrow \dots$ which is induced by the expansion g . For each point $a = (a_0, a_1, \dots) \in \Sigma$, define $h(a) = (g(a_0), a_0, a_1, \dots)$. Then $h: \Sigma \rightarrow \Sigma$ is a homeomorphism. By the

definition given by Williams, Σ is called a solenoid with a shift map h . The dynamics $(\Lambda_f, f|_{\Lambda_f})$ and (Σ, h) are conjugate, by the homeomorphism

$$P: \Lambda_f \rightarrow \Sigma, \quad x \mapsto (p(x), p(f^{-1}(x)), p(f^{-2}(x)), \dots), \quad \text{for all } x \in \Lambda_f.$$

DEFINITION 2.4. A diagram \mathcal{D} on an orientable closed surface S is a finite collection of simple closed curves intersecting transversely in S .

Two diagrams \mathcal{D}_1 and \mathcal{D}_2 on S are isotopic if there is an isotopy of S that carries \mathcal{D}_1 to \mathcal{D}_2 . Isotopic diagrams will be thought as the same one.

Two diagrams \mathcal{D}_1 and \mathcal{D}_2 on S are homeomorphic, denoted by $\mathcal{D}_1 \simeq \mathcal{D}_2$, if there is a homeomorphism $h: S \rightarrow S$ such that $h(\mathcal{D}_1) = \mathcal{D}_2$.

For any closed orientable 3-manifold M , there is an orientable closed sub-surface S splitting M into two handlebodies N_1 and N_2 . In this paper, we only consider the splitting with S having genus two. Hence for each N_i we can find disjoint simple closed curves $\alpha_i, \beta_i, \gamma_i$ in S such that they all bound disks in N_i , γ_i is a separating curve, α_i and β_i are non-separating and lie on different sides of γ_i . Then $\{\alpha_1, \beta_1, \gamma_1\}$ together with $\{\alpha_2, \beta_2, \gamma_2\}$ form a diagram on S .

DEFINITION 2.5. We call the diagram $\{\alpha_1, \beta_1, \gamma_1\} \cup \{\alpha_2, \beta_2, \gamma_2\}$ an alternating Heegaard diagram if each curve of $\{\alpha_i, \beta_i, \gamma_i\}$ intersect $\{\alpha_j, \beta_j, \gamma_j\}$ in the cyclic order

$$\alpha_j, \gamma_j, \beta_j, \gamma_j, \alpha_j, \gamma_j, \beta_j, \gamma_j, \dots, \quad i \neq j.$$

We call a Heegaard splitting alternating if it admits an alternating Heegaard diagram.

As an example, Figure 3 shows an alternating Heegaard diagram. By the discussions in Sections 3 and 4, we will see that this diagram gives us the Prism manifold $P(1, 2)$.

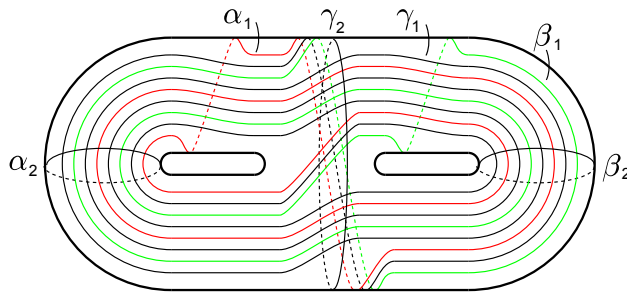


FIGURE 3. Alternating Heegaard diagram.

REMARK 2.6. (a) In the classical definition of Heegaard diagram, γ_i may be omitted.

(b) The above definition of alternating Heegaard splitting coincides with the definition of “alternating Heegaard splitting of type I” in [5].

(c) If we just require $\{\alpha_1, \beta_1, \gamma_1\}$ to be disjoint simple closed curves in S such that they intersect $\{\alpha_2, \beta_2, \gamma_2\}$ as in Definition 2.5, then one can show that γ_1 must be separating, α_1 and β_1 are non-separating and lie on different sides of γ_1 .

2.2. Construction of the diffeomorphism f . Suppose $M = N_1 \cup_S N_2$ is a genus two alternating Heegaard splitting, with an alternating Heegaard diagram $\{\alpha_1, \beta_1, \gamma_1\} \cup \{\alpha_2, \beta_2, \gamma_2\}$. Then we can construct $f \in \text{Diff}(M)$ as follows. For more details one can see [3] and [5].

Firstly we give N_i , a “disk fibre bundle” structure, fibred over the branched manifold K , such that $\alpha_i, \beta_i, \gamma_i$ are all boundaries of fibres. Let p_i be the corresponding projection map. We choose a spine K_i in N_i as in Figure 4 (a), then $p_i|_{K_i} : K_i \rightarrow K$ is an immersion as in Figure 4 (b).

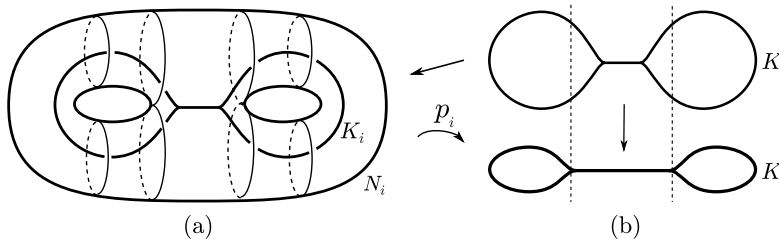


FIGURE 4. Spine in N_i .

Then we choose three points $x_\alpha, x_\beta, x_\gamma$ separately in $\alpha_1 \cap \alpha_2, \beta_1 \cap \beta_2, \gamma_1 \cap \gamma_2$, and add three half twist bands between “edges” of K_i and $\alpha_j, \beta_j, \gamma_j, i \neq j$. The “core” of each band should contain a chosen point and lie in a fibre. The half twists from different sides should have the same “direction”. Figure 5 (a) shows the three bands in N_2 and Figure 5 (b) shows that two bands from different sides intersect at a chosen point.

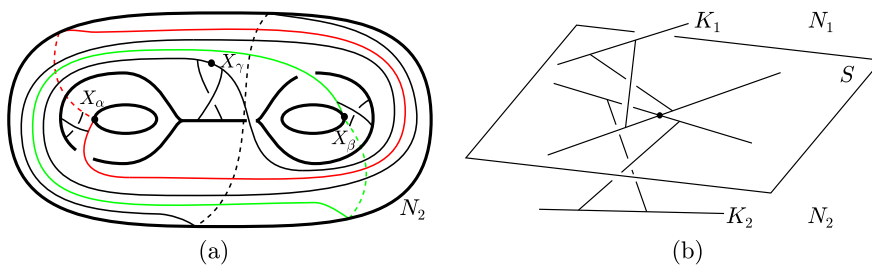


FIGURE 5. Adding bands on spines.

We can get two new branched manifolds, and one of them is as in Figure 6 (a). Then we push them into N_i to get K'_i as in Figure 6 (b). We can require that

$p_i|_{K'_i}: K'_i \rightarrow K$ is also an immersion. Denote the regular neighbourhoods of K_i and K'_i by $N(K_i)$ and $N(K'_i)$, which are all contained in N_i and have induced “disk fibre bundle” structure. We construct the required $f \in \text{Diff}(M)$ in three steps.

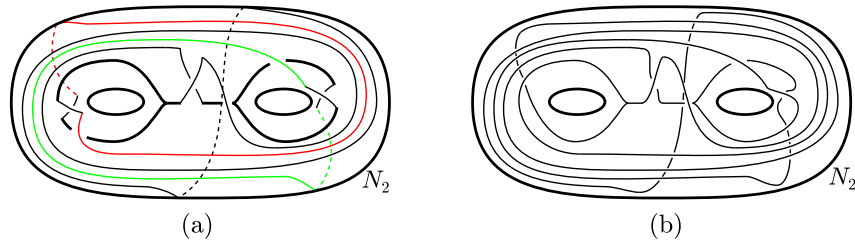


FIGURE 6. New branched manifold in handlebody.

STEP 1. There is $f_1 \in \text{Diff}(M)$ which is isotopic to the identity, fixing $N(K'_1)$ and on N_2 it satisfies the *contracting condition on fibres*, mapping N_2 to $N(K_2)$, see Figure 7.

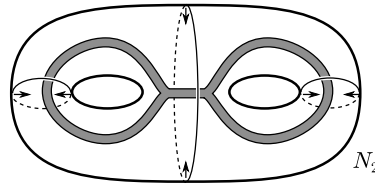


FIGURE 7. Contraction on fibres.

STEP 2. Via suitable isotopy, we can move K_2 and its neighbourhood $N(K_2)$ along the bands in N_2 , see Figure 8 (b). Since $\alpha_2, \beta_2, \gamma_2$ bound disjoint disks in N_2 , we can then move K'_1 and its neighbourhood $N(K'_1)$ along those disks, see Figure 8 (c). And we can further move them to the position as in Figure 8 (d).

Then since $\alpha_1, \beta_1, \gamma_1$ bound disjoint disks in N_1 , we can move K_2 and $N(K_2)$ further along these disks to K'_2 and $N(K'_2)$, see Figure 8 (e). And finally we can move K'_1 and $N(K'_1)$ to K_1 and $N(K_1)$, see Figure 8 (f). Combining these moves we get $f_2 \in \text{Diff}(M)$, which is isotopic to the identity.

$f_2|_{N(K'_1)}: N(K'_1) \rightarrow N(K_1)$ and $f_2|_{N(K_2)}: N(K_2) \rightarrow N(K'_2)$ can be chosen to be fibre preserving. If we let g_1 and g_2 denote their induced maps on K , then f_2 can be further chosen such that g_1^{-1} and g_2 satisfy the *expanding condition on K* .

STEP 3. There is $f_3 \in \text{Diff}(M)$ which is isotopic to the identity, fixing $N(K'_2)$ and on N_1 its inverse f_3^{-1} satisfies the *contracting condition on fibres*, mapping N_1 to $N(K_1)$. On $N(K_1)$ the map f_3 is as in Figure 9.

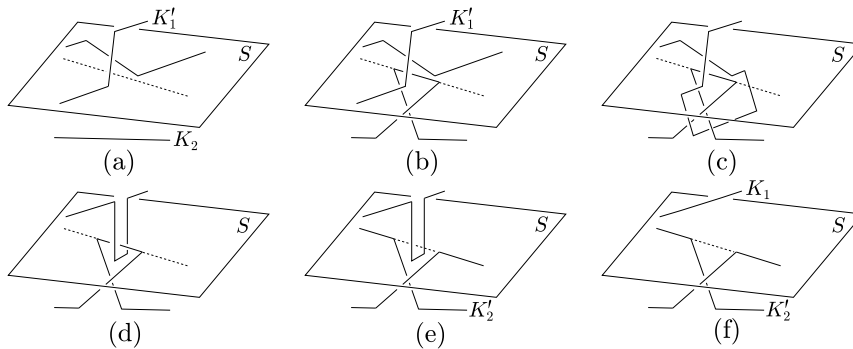


FIGURE 8. Isotopy of K_1 and K_2 .

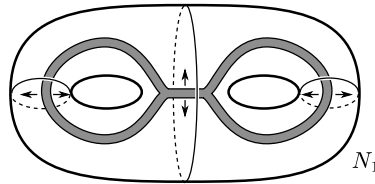


FIGURE 9. Expansion on fibres.

Let $f = f_3 \circ f_2 \circ f_1 \in \text{Diff}(M)$, by the construction, f is isotopic to the identity. It is easy to see $\Omega(f) = \bigcap_{i=1}^{\infty} f^i(N_2) \cup \bigcap_{i=1}^{\infty} f^{-i}(N_1)$ is a union of two Williams solenoids. And clearly the Williams solenoids derived from alternating Heegaard splittings (defined as in Definition 2.5) are all handcuffs solenoids.

3. Alternating Heegaard diagram

Suppose $\{\alpha_1, \beta_1, \gamma_1\} \cup \{\alpha_2, \beta_2, \gamma_2\}$ is an alternating Heegaard diagram on a splitting surface S . We can assume the curves $\{\alpha_2, \beta_2, \gamma_2\}$ are in the standard position like in Figure 3. We color the curves $\{\alpha_1, \beta_1, \gamma_1\}$ separately by red, green and black. Then the red (green) curve is non-separating, the black curve is separating.

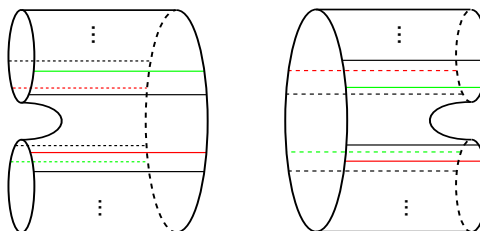


FIGURE 10. Two 3-punctured spheres.

Cutting S along $\{\alpha_2, \beta_2, \gamma_2\}$, we get two 3-punctured spheres S_l and S_r . Since $\{\alpha_1, \beta_1, \gamma_1\}$ intersect $\{\alpha_2, \beta_2, \gamma_2\}$ in the cyclic order $\alpha_2, \gamma_2, \beta_2, \gamma_2, \dots$, the colored curves must be cut into arcs lying in S_l and S_r . Moreover, it can be “straightened” as in Figure 10. Clearly colored arcs in S_l and S_r have the same number. Since $\{\alpha_2, \beta_2, \gamma_2\}$ intersect $\{\alpha_1, \beta_1, \gamma_1\}$ in the cyclic order $\alpha_1, \gamma_1, \beta_1, \gamma_1, \dots$, this number can be divided by 8.

The original diagram can be obtained from Figure 10 by pasting the cuts. There is a quite natural way to paste the cuts as in Figure 11 which contains $4n$ ($n > 0$) (non-colored) parallel simple closed curves. Hence the original diagram can be thought of as obtained from Figure 11 by some “twist” operations.

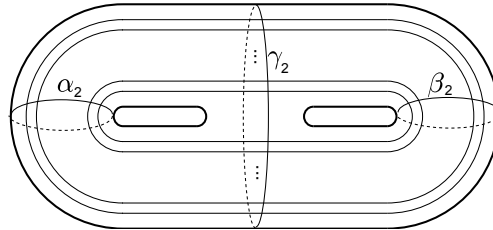


FIGURE 11. Trivial diagram.

DEFINITION 3.1. Let \mathcal{D} be a diagram on an oriented closed surface S , c be a simple closed curve in S which intersects \mathcal{D} transversely. Then we have a local picture as in Figure 12 (a). The twist operation \mathcal{T}_c on \mathcal{D} is as in Figure 12 (b). It is invertible.

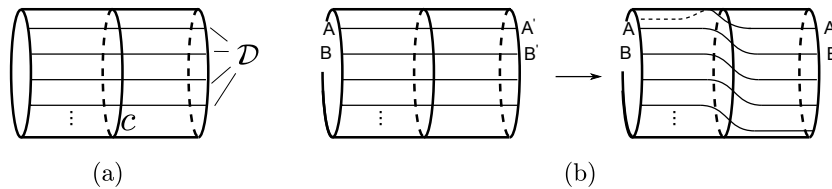


FIGURE 12. Local model and twist operation.

If we look from positive side of S , \mathcal{T}_c is a right-hand shift along c , and \mathcal{T}_c^{-1} is a left-hand shift along c .

REMARK 3.2. \mathcal{T}_c is an operation on diagrams. Do not confuse it with the Dehn twist t_c , which is an automorphism of S and normally can be defined as in Figure 13. Out of the annulus neighbourhood of c , t_c is the identity. On the annulus t_c is like a left hand 2π -twist. Its inverse t_c^{-1} is like a right hand 2π -twist.

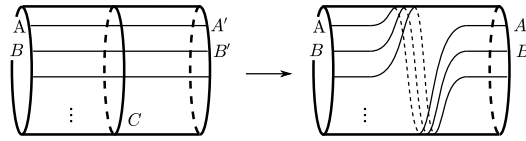


FIGURE 13. Dehn twist.

DEFINITION 3.3. Define $D(4n; 0, 0, 0)$ to be the diagram as in Figure 11 which consists of $4n$ parallel curves and $\{\alpha_2, \beta_2, \gamma_2\}$. Pushing each curve of $\{\alpha_2, \beta_2, \gamma_2\}$ slightly to either side we get their parallel curves $\{c_1, c_2, c_3\}$. Then \mathcal{T}_{c_i} are mutually commutative. Define $D(4n; m_1, m_2, m_3)$ to be $\mathcal{T}_{c_1}^{m_1} \mathcal{T}_{c_2}^{m_2} \mathcal{T}_{c_3}^{m_3}(D(4n; 0, 0, 0))$, here m_i are all integers.

From the above discussion we have:

LEMMA 3.4. Any alternating Heegaard diagram has the form

$$D(4n; m_1, m_2, m_3).$$

LEMMA 3.5. For $D(4n; m_1, m_2, m_3)$, we have following homeomorphisms:

- (a) $D(4n; m_1, m_2, m_3) \simeq D(4n; m'_1, m'_2, m'_3)$, $m_i \equiv m'_i \pmod{4n}$.
- (b) $D(4n; m_1, m_2, m_3) \simeq D(4n; m_2, m_1, m_3)$.
- (c) $D(4n; m_1, m_2, m_3) \simeq D(4n; -m_1, -m_2, -m_3)$.

PROOF. We can put arcs in S_l and S_r in a symmetric way as in Figure 10, then paste the cuts “symmetrically” to obtain the diagrams. These homeomorphisms can be obtained by Dehn twist (half twist), π -rotation and reflection as in Figure 14.

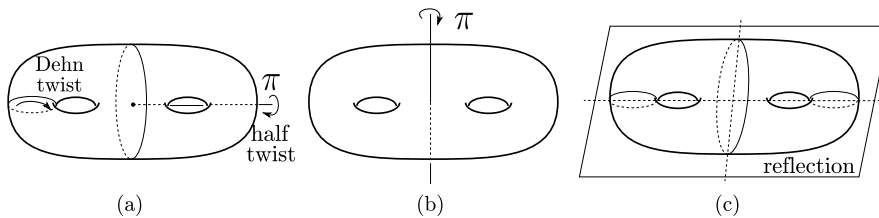


FIGURE 14. Symmetries of diagrams.

We also have the following lemma which can be easily proved.

LEMMA 3.6. The Dehn twist (half twist), π -rotation and reflection as in Figure 14 map an alternating Heegaard diagram to an alternating Heegaard diagram.

THEOREM 3.7. The diagram $D(4n; m_1, m_2, m_3)$ is an alternating Heegaard diagram if and only if $(m_1, m_2, m_3) = \eta + 4(k_1, k_2, k_3)$, here η is one of the following integral vectors $\pm(1, -3, 1)$, $\pm(1, -5, 2)$, k_i are all integers and satisfy $(n, k_1 + k_2 + 2k_3) = 1$.

PROOF. *The Only If Part.* Suppose $D(4n; m_1, m_2, m_3)$ is alternating. Cut S along $\{\alpha_2, \beta_2, \gamma_2\}$ as before, then we get S_l and S_r . We first look at S_l .

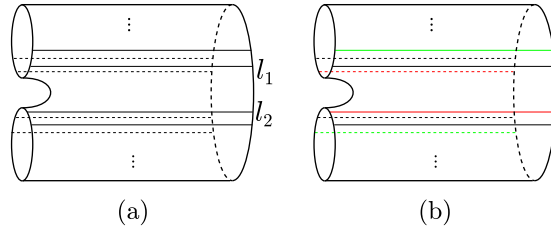


FIGURE 15. Uncolored and colored left surfaces.

By Definition 2.5, it is easy to see that one of l_1 and l_2 must be black. By Lemmas 3.5 and 3.6, we can assume l_1 is black, otherwise we consider the reflection image of this diagram. Then we can further assume l_2 is red, otherwise we recolor the curves α_1 and β_1 . Hence by Definition 2.5, S_l should be as in Figure 15 (b).

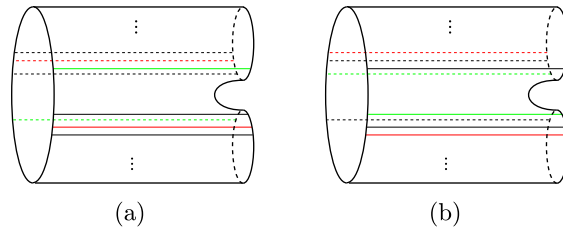


FIGURE 16. Two possible right surfaces.

The situation of S_r should be similar. If we cut S_l and S_r further along all black arcs, then only the piece containing the saddle can contain two arcs with the same color red or green. Other pieces are all rectangles containing only one arc. Hence for S_r the piece containing the saddle must contain two green arcs, otherwise β_1 will be parallel to γ_1 . Then by Definition 2.5, we have two possibilities of S_r as in Figure 16.

CASE 1. S_r is as in Figure 16 (a).

We fix a base position $\eta = (1, -3, 1)$. This means that if before cutting along $\{\alpha_2, \beta_2, \gamma_2\}$ the diagram is $D(4n; 1, -3, 1)$, then colors of the arcs will be coincident at the cuts. $D(4n; m_1, m_2, m_3)$ can be obtained from $D(4n; 1, -3, 1)$ by twist operations, hence clearly $(m_1, m_2, m_3) = \eta + 4(k_1, k_2, k_3)$.

In S , colored curves intersect γ_2 at $8n$ points, $2n$ red points, $2n$ green points and $4n$ black points, along γ_2 in the cyclic order red, black, green, black, ... Looking at γ_2 from left to right, give the red (green) points which belong to the saddle piece a symbol 0 ($0'$) and other red (green) points symbols $1, \dots, n - 1$

$(1', \dots, n - 1')$ clockwise, then the picture will be as in Figure 17 (a), $\bar{k}_3 \equiv k_3 \pmod{n}$, $0 \leq \bar{k}_3 < n$.

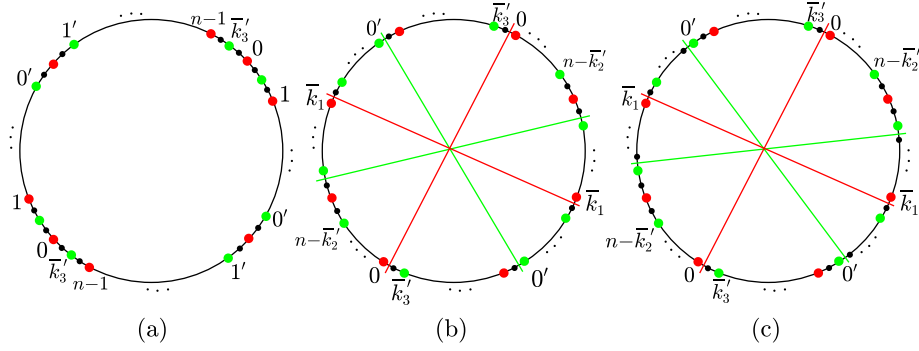


FIGURE 17. Equivalence relation on points in γ_2 .

We define an equivalence relation on the black (red, green) points in γ_2 , which is generated by the following two relations:

\tilde{R}_l : two black (red, green) points are equivalent if arcs in S_l containing them have a common boundary in α_2 .

\tilde{R}_r : two black (red, green) points are equivalent if arcs in S_r containing them have a common boundary in β_2 .

There are four open sectors with red (green) boundaries as in Figure 17 (b). Here $\bar{k}_i \equiv k_i \pmod{n}$, $0 < \bar{k}_2 \leq n$, $0 \leq \bar{k}_1, \bar{k}_3 < n$, the red (green) lines pass through the midpoints of the red (green) points and their neighbour black points. It can be checked that reflections on γ_2 which interchange two red (green) non-adjacent sectors give us \tilde{R}_l (\tilde{R}_r) on the black (red, green) points in those sectors.

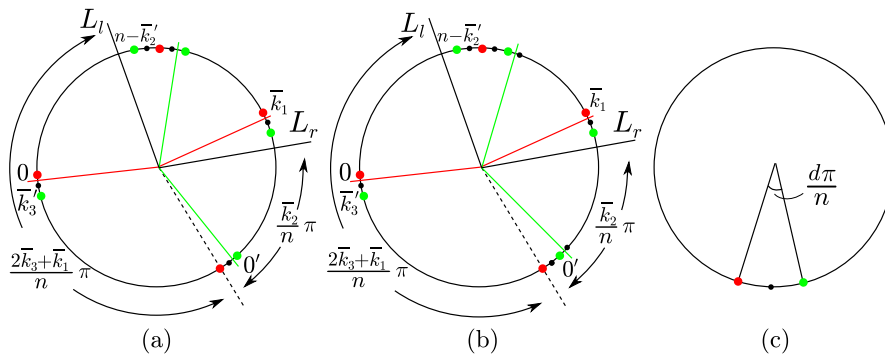


FIGURE 18. Reflections and quotient space.

Then the equivalence relation induces an equivalence relation on black (red, green) points in RP^1 . Here RP^1 is obtained by identifying antipodal points

of γ_2 . This induced equivalence relation is generated by two reflections R_l and R_r with reflection lines L_l and L_r as in Figure 18 (a).

By the connectedness of the black (red, green) curve, all black (red, green) points in γ_2 are equivalent. Hence the dihedral group generated by R_l and R_r acts transitively on the black (red, green) points in RP^1 . In Figure 18 (a), let θ denote the angle between L_l and L_r , then $\theta \equiv \pm(k_1 + k_2 + 2k_3)\pi/n \pmod{\pi}$. Notice that L_l and L_r only pass through red or green points.

CLAIM 3.8. *The group generated by R_l and R_r acts transitively on black (both red and green) points in RP^1 if and only if $(n, k_1 + k_2 + 2k_3) = 1$.*

PROOF OF CLAIM. Let $(n, k_1 + k_2 + 2k_3) = d$, then modulo the group action we get a corner with boundaries containing red or green points and having angle $d\pi/n$. Hence the group acts transitively on black (both red and green) points if and only if $d = 1$, see Figure 18 (c). □

Hence we finish the discussion of Case 1.

CASE 2. S_r is as in Figure 16 (b).

We fix a base position $\eta = (1, -5, 2)$ similar to Case 1. Then as above we have $(m_1, m_2, m_3) = \eta + 4(k_1, k_2, k_3)$. The following discussion is exactly the same as in Case 1, except that instead of Figures 17 (b) and 18 (a) we will get Figures 17 (c) and 18 (b), and we have $(n, k_1 + k_2 + 2k_3) = 1$.

The If Part. Suppose $(m_1, m_2, m_3) = \eta + 4(k_1, k_2, k_3)$, η is one of $\pm(1, -3, 1)$, $\pm(1, -5, 2)$ and $(n, k_1 + k_2 + 2k_3) = 1$. By Lemmas 3.5 and 3.6, we can assume η is $(1, -3, 1)$ or $(1, -5, 2)$. Cut $D(4n; m_1, m_2, m_3)$ along $\{\alpha_2, \beta_2, \gamma_2\}$, then we get S_l and S_r .

Clearly we can color the arcs in S_l as in Figure 15 (b). Then we can color S_r as in Figure 16 (a) or Figure 16 (b) according to whether η is $(1, -3, 1)$ or $(1, -5, 2)$. Then the colors of those arcs will coincide at points in $\{\alpha_2, \beta_2, \gamma_2\}$. Hence we can have equivalence relations on black (red, green) points in γ_2 and black (red, green) points in RP^1 as in the proof of The Only If Part.

Since $(n, k_1 + k_2 + 2k_3) = 1$, by Claim, all black (red, green) points in RP^1 are equivalent. Hence there are at most two equivalence classes of black (red, green) points in γ_2 , and in S we have at most two black (red, green) curves.

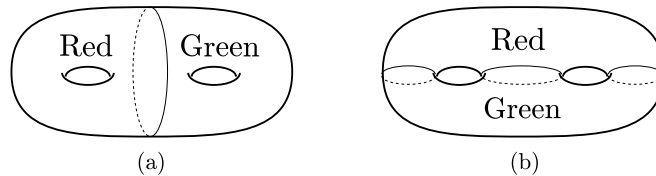


FIGURE 19. Red and green surfaces.

Notice that there is a pair of red (green) antipodal points in γ_2 lying in the saddle piece of S_l (S_r). Hence the union of pieces containing the red (green) arcs is a connected subsurface in S , with Euler characteristic -1 . Hence there are two possible cases as in Figure 19.

Since there are at most two black curves, we meet the case Figure 19 (a), and there is only one black curve which is separating. Then the red (green) curve is non-separating because the two sides of it can be connected by a parallel curve of the black curve. Hence there are only one red curve and one green curve, both non-separating. \square

4. Manifolds with alternating Heegaard splittings

DEFINITION 4.1. Let $\eta_1 = (1, -3, 1)$, $\eta_2 = (1, -5, 2)$. Let $M_i(n; k_1, k_2, k_3)$ be the 3-manifold which has an alternating Heegaard diagram $D(4n; m_1, m_2, m_3)$ with $(m_1, m_2, m_3) = \eta_i + 4(k_1, k_2, k_3)$, $i = 1, 2$. Here $n > 0$, $(n, k_1 + k_2 + 2k_3) = 1$.

LEMMA 4.2. *If a 3-manifold M admits an alternating Heegaard splitting, then M must be homeomorphic to some $M_i(n; k_1, k_2, k_3)$ with the inequalities $0 < k_2 \leq n$, $0 \leq k_3 < n$ and $n \leq k_1 + k_2 + 2k_3 < 2n$.*

PROOF. If two Heegaard diagrams are homeomorphic, then they give the homeomorphic 3-manifolds. Then, by Theorem 3.7 and Lemma 3.5, we get the results. \square

In what follows we identify some of $M_1(n; k_1, k_2, k_3)$ and $M_2(n; k_1, k_2, k_3)$ as in Lemma 4.2 to our familiar 3-manifolds. Notice that every alternating Heegaard diagram admits an involution τ which preserves the black (red, green) curve, as in Figure 20.

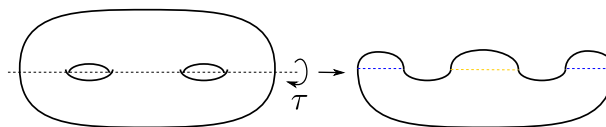


FIGURE 20. Involution and branched cover.

PROPOSITION 4.3. $M_1(n; k_1, k_2, k_3)$ ($M_2(n; k_1, k_2, k_3)$) as in Lemma 4.2 is a 2-fold branched cover of S^3 . The branched set is a three bridge link. It consists of a blue two bridge link and a yellow trivial circle as in Figure 21 (a) (21 (b)). The front (back) blue arcs lying in the surface of the $n \times n$ square pillow have slope $-m/n(m/n)$, $m = k_1 + k_2 + 2k_3 - n$. In the front square, walking from the point B to the left we get the arc L_s . Walking along the oriented circle c from L_s by $2k_3$ we get the arc L_t . Hence the position of the yellow circle can be determined. As an example, Figure 21 (c) shows the corresponding branched set of $M_1(5; 2, 3, 1)$.

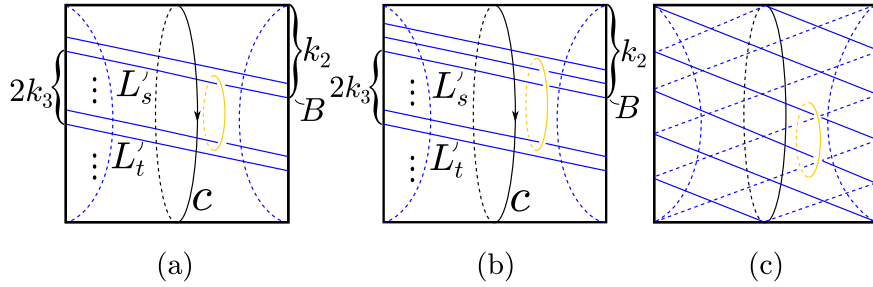


FIGURE 21. Three bridge links.

PROOF. Let $M_1(n; k_1, k_2, k_3) = N_1 \cup_S N_2$ as before. On N_2 the branched cover is given by the involution τ as in Figure 20. It induces a branched cover of the black (red, green) curve. On γ_2 it is a π -rotation and on α_2 and β_2 it is a reflection. These reflections are essentially R_l and R_r defined on RP^1 in the proof of Theorem 3.7, see Figure 18. Since the reflection lines L_l and L_r only pass red or green points, we know that on the black curve τ is a π -rotation and on the red (green) curve τ is a reflection.

Cut N_2 open along disks bounded by α_2 and β_2 . Modulo the involution, we get a cylinder as in Figure 22 (a). Then modulo reflections on the left and right disks we get N_2/τ , an $n \times n$ square pillow as in Figure 22 (b). With suitable twists, we can require that the front arcs have slope $-m/n$ and the back arcs have slope m/n . And the position of the yellow arc is as in Figure 21 (a).

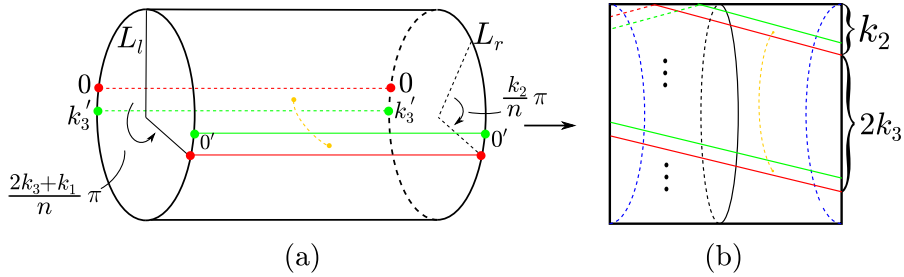


FIGURE 22. Cylinder and square pillow.

Let N_1 be as in Figure 23 (a). We can extend τ to a π -rotation (reflection) on the disk bounded in N_1 by the black (red, green) curve. Hence we can further extend τ to the whole N_1 and get the N_1/τ as in Figure 23 (b).

Clearly, $M_1(n; k_1, k_2, k_3)/\tau = N_1/\tau \cup_{S/\tau} N_2/\tau$ is S^3 with branched set a three bridge link that consists of a blue link and a yellow circle. We can push the blue arcs in N_1/τ across the disks to the red and green arcs, then the yellow arc is

just a trivial arc in N_1/τ . For $M_2(n; k_1, k_2, k_3)$ the discussion is similar, and we finish the proof. \square

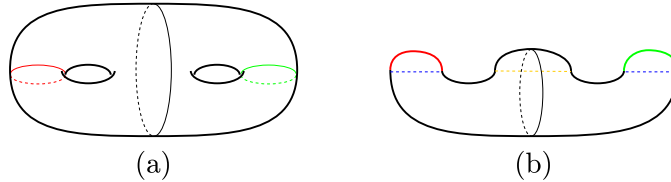


FIGURE 23. Involution on N_1 .

PROPOSITION 4.4. Let $M_1(n; k_1, k_2, k_3)$ ($M_2(n; k_1, k_2, k_3)$) be as in Lemma 4.2 and $m = k_1 + k_2 + 2k_3 - n$. We have the following homeomorphisms:

- (a) $M_1(n; k_1, k_2, 0) \simeq L(n, m) \# S^1 \times S^2, 0 \leq m < n$.
- (b) $M_2(n; k_1, k_2, 0) \simeq L(n, m) \# L(2, 1), 0 \leq m < n$.
- (c) $M_1(n; 0, n - m, m) \simeq P(m, n), 0 < m < n$.
- (d) $M_2(n; m - 1, n - 2m + 1, m) \simeq S^2(-1/2, 1/4, m/n), 0 < m < n/2$.

PROOF. The proof depends on Proposition 4.3 and the fact that the 2-fold branched cover of a Montesinos link is a Seifert fibred space. Moreover, an (m, n) -rational tangle corresponds to a singular fibre with invariant m/n . This can be found, for example, in Chapters 11 and 12 of [2].

In what follows we identify the 2-fold branched covers of the corresponding links of M_1 and M_2 in the proposition. Considering Figure 21, since the yellow arc in N_1/τ is a trivial arc, we can push it into S/τ disjoint from the blue arcs. Then we further push it into the square pillow. Hence it is contained in a smaller box, as in Figure 24 (a).

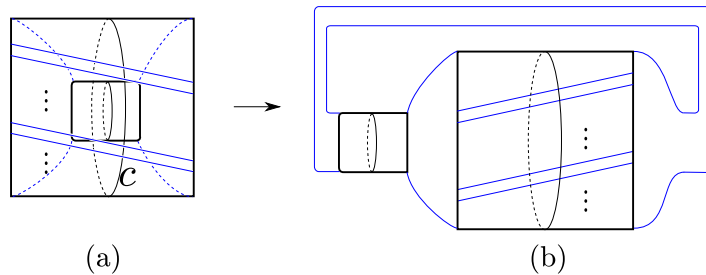


FIGURE 24. Two boxes.

After a π -rotation about the circle c we change the outside and inside of the square pillow, and we redraw it as in Figure 24 (b). Now the left box contains the yellow circle and two blue arcs, and the right box is exactly an (m, n) -rational tangle.

When $k_3 = 0$, the picture is as in Figure 25. The three bridge link can be written as a connected sum of a two bridge link and a 2-component trivial link (or a Hopf link). The connected sum of links corresponds to the connected sum of their 2-fold branched covers. The 2-fold branched cover of a 2-component trivial link (or a Hopf link) is $S^1 \times S^2$ (or RP^3). The 2-fold branched cover of the blue two bridge link in Figure 25 (a) is $L(n, m)$. Hence we get the first two homeomorphisms.

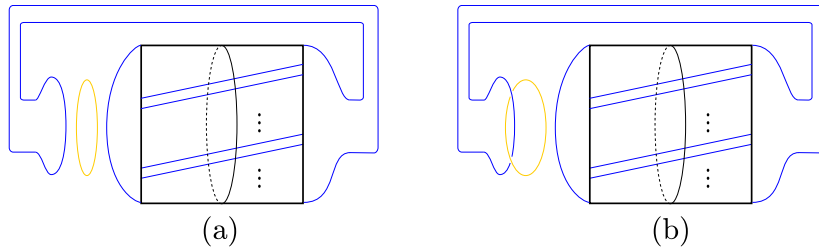


FIGURE 25. Connected sums.

To show the last two homeomorphisms, we redraw the corresponding links in Figure 26. Figures 26 (a)(c) give us the pictures when we push the yellow arc in N_1/τ into S/τ . Figures 26 (b)(d) show us how the links will be look like after we perform the procedure as in Figure 24.

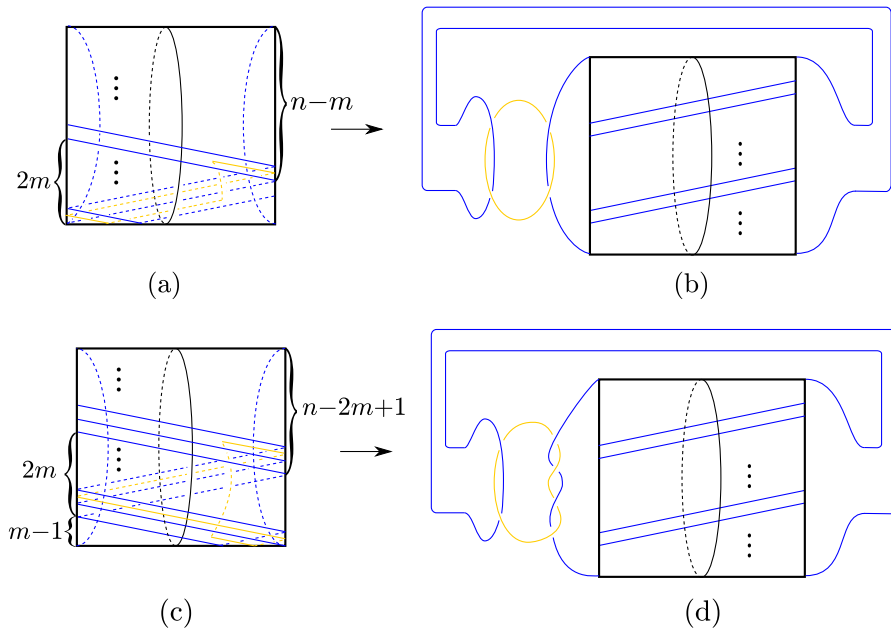


FIGURE 26. Montesinos links.

These two links are all Montesinos links with three rational tangles. For Figure 26 (b), the three rational tangles have parameters $(-1, 2), (1, 2)$ and (m, n) . For Figure 26 (d), the three rational tangles have parameters $(-1, 2), (1, 4)$ and (m, n) . Hence 2-fold branched covers of these two links are all Seifert fibred spaces, and the invariants are exactly as in the proposition. \square

PROPOSITION 4.5. $M_2(n; 0, n - 3, 2)$ ($n \geq 5$) has a 2-fold cover which is homeomorphic to some Dehn surgery on the hyperbolic link 6_3^2 . $M_2(n; 0, n - 3, 2)$ are all hyperbolic 3-manifolds, except for finitely many n .

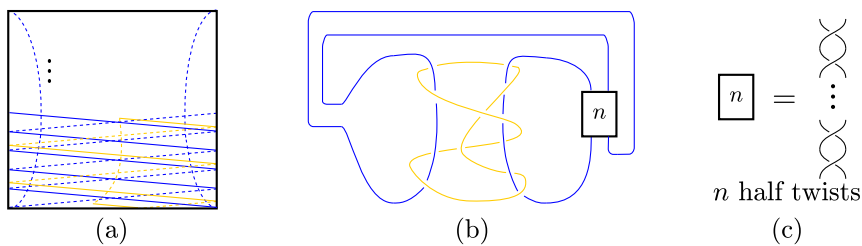


FIGURE 27. The quotient $M_2(n; 0, n - 3, 2)/\tau$.

PROOF. The manifold $M_2(n; 0, n - 3, 2)$ ($n \geq 5$) is the 2-fold branched cover of the link as in Figure 27 (a). As in the proof of Proposition 4.4, this link is isotopic to the link in Figure 27 (b), here the n -box denotes two parallel vertical singular arcs with n half twists as in Figure 27 (c).

If we replace the n -box by a box containing two parallel horizontal singular arcs, then the picture will be as in Figure 28 (a), which is a Hopf link. The new box can be thought of as a regular neighbourhood of a regular arc. We can move this picture to the position as in Figure 28 (b).

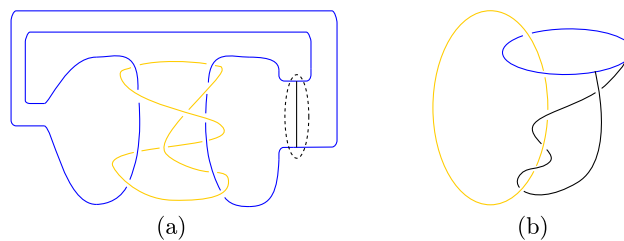


FIGURE 28. Surgery on $M_2(n; 0, n - 3, 2)/\tau$.

Clearly the 2-fold branched covers of the new box and the original n -box are solid tori. Since the 2-fold branched cover of the Hopf link is RP^3 , we know that $M_2(n; 0, n - 3, 2)$ is some Dehn surgery on a knot in RP^3 . When we consider a further 2-fold cover, the knot becomes the link 6_3^2 in S^3 .

This can be easily seen from another way to get the 4-fold branched cover as follows. Figure 29 (a) is the 2-fold branched cover of Figure 28 (b). Figure 29 (b) is isotopic to Figure 29 (a). Figure 29 (c) is the 2-fold branched cover of Figure 29 (b).

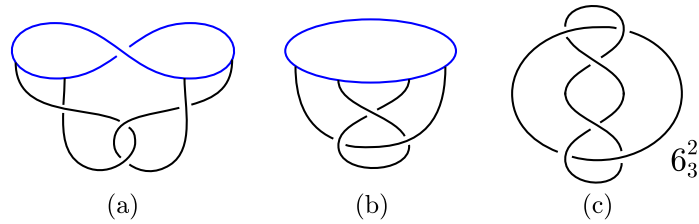


FIGURE 29. Branched covers and the link 6_3^2 .

The link 6_3^2 is hyperbolic. One can show that its quotient knot in RP^3 is also hyperbolic. Then by Thurston’s Hyperbolic Dehn Surgery Theorem, all surgeries are hyperbolic 3-manifolds, except for finitely many cases (see [8]). \square

REMARK 4.6. Since the orbifold $M_2(n; 0, n - 3, 2)/\tau$ has 1-dimensional singular set, one can also use the Orbifold Theorem to get the results (see [1]).

5. Weakly alternating Heegaard diagram

Suppose $M = N_1 \cup_S N_2$ is a genus two Heegaard splitting. The disjoint simple closed curves $\alpha_i, \beta_i, \gamma_i$ in S bound disks in N_i . γ_i is a separating curve, α_i and β_i are non-separating and lie on different sides of γ_i .

DEFINITION 5.1. We call the diagram $\{\alpha_1, \beta_1, \gamma_1\} \cup \{\alpha_2, \beta_2, \gamma_2\}$ a weakly alternating Heegaard diagram if γ_i intersects $\{\alpha_j, \beta_j, \gamma_j\}$ in the cyclic order

$$\alpha_j, \gamma_j, \beta_j, \gamma_j, \alpha_j, \gamma_j, \beta_j, \gamma_j, \dots, \quad i \neq j.$$

We call a Heegaard splitting weakly alternating if it admits a weakly alternating Heegaard diagram.

REMARK 5.2. Suppose $\{\alpha_1, \beta_1, \gamma_1\} \cup \{\alpha_2, \beta_2, \gamma_2\}$ is weakly alternating and $\{\alpha_1, \beta_1, \gamma_1\}$ does not intersect $\{\alpha_2, \beta_2, \gamma_2\}$ minimally, then there is a bi-gon in some $\alpha_i \cup \beta_j$ ($i \neq j$). We can move α_i or β_j to get a new weakly alternating Heegaard diagram with fewer intersections, and not to affect the corresponding 3-manifold. Hence further we only consider weakly alternating Heegaard diagrams with minimal intersections.

Clearly an alternating Heegaard diagram is weakly alternating. Figure 30 shows a weakly alternating Heegaard diagram which is not alternating. In Section 6, we will see that this diagram gives us the Poincaré’s homology 3-sphere

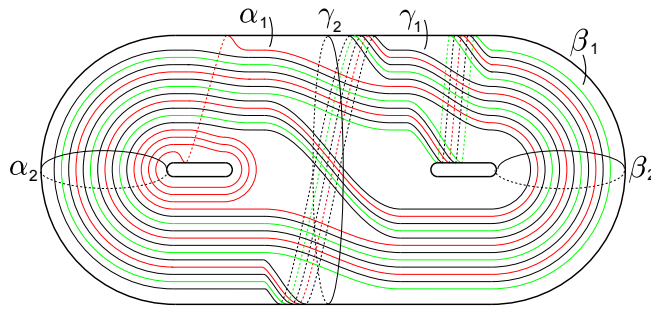


FIGURE 30. Weakly alternating Heegaard diagram.

$S(-1/2, 1/3, 1/5)$, which does not admit any alternating Heegaard splitting. Now we give a proof of Theorem 1.2.

PROOF OF THEOREM 1.2. Similar to the construction part in Section 2, now we choose only one point x_γ in $\gamma_1 \cap \gamma_2$ and add only one band in N_i connecting K_i and γ_j , $i \neq j$. Then we can similarly get $K'_i, N(K_i), N(K'_i)$ and f_1, f_2, f_3 .

Notice that still we can choose f_2 such that the induced maps g_1^{-1} and g_2 satisfy the *expanding condition on K* , because in Figure 4 one can see that the loops have been drawn longer and after the isotopy the middle arc will also be longer. Actually we can make a small modification on K'_i as in Figure 31, and correspondingly modify f_2 by further isotopy. Then the expansion on K will be more clear.

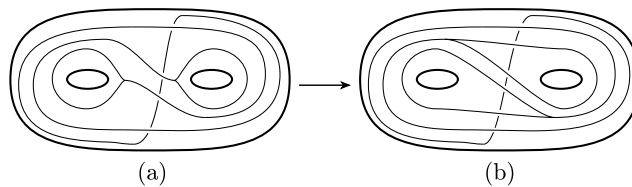


FIGURE 31. Expansion of the spine.

Following the construction Steps 1–3 in Section 2, we can get the required f . \square

REMARK 5.3. By the proof, it is clear that the Williams solenoids derived from weakly alternating Heegaard splittings are all handcuffs solenoids.

Suppose $D(4n; m_1, m_2, m_3) = \{\alpha_1, \beta_1, \gamma_1\} \cup \{\alpha_2, \beta_2, \gamma_2\}$ is an alternating Heegaard diagram. Let c_i ($1 \leq i \leq 5$) be simple closed curves in S as in Figure 32. And let t_{c_i} ($1 \leq i \leq 5$) denote the Dehn twist along c_i as in Remark 3.2.

DEFINITION 5.4. Let l and r be two integers. Define $D(4n; m_1[l], m_2[r], m_3)$ to be the diagram $t_{c_4}^l t_{c_5}^r (\{\alpha_1, \beta_1, \gamma_1\} \cup \{\alpha_2, \beta_2, \gamma_2\})$. If l or r is 0, the diagram will also be denoted by $D(4n; m_1, m_2[r], m_3)$ or $D(4n; m_1[l], m_2, m_3)$. Clearly

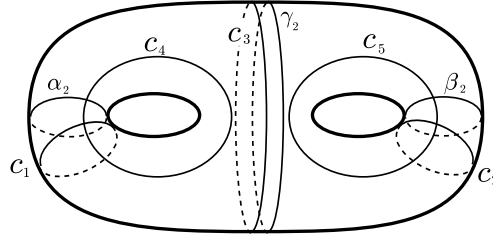


FIGURE 32. Simple closed curves in S .

$D(4n; m_1[0], m_2[0], m_3)$ is the same as $D(4n; m_1, m_2, m_3)$, the alternating Heegaard diagram itself.

LEMMA 5.5. *If $D(4n; m_1, m_2, m_3)$ is alternating, then $D(4n; m'_1, m'_2, m'_3)$, $D(4n; m_2, m_1, m_3)$, $D(4n; -m_1, -m_2, -m_3)$ and $D(4n; -m_1, m_2, m_1 + m_3)$ are alternating, here $m'_i \equiv m_i \pmod{4n}$. Moreover, we have following homeomorphisms:*

- (a) $D(4n; m_1[l], m_2[r], m_3) \simeq D(4n; m_1[l], m_2[r], m'_3)$, $m_3 \equiv m'_3 \pmod{4n}$.
- (b) $D(4n; m_1[l], m_2[0], m_3) \simeq D(4n; m_1[l], m'_2[0], m_3)$, $m_2 \equiv m'_2 \pmod{4n}$.
- (c) $D(4n; m_1[l], m_2[r], m_3) \simeq D(4n; m_2[r], m_1[l], m_3)$.
- (d) $D(4n; m_1[l], m_2[r], m_3) \simeq D(4n; -m_1[-l], -m_2[-r], -m_3)$.

If further $0 < m_1 < 4n$, we have the following homeomorphism:

- (e) $D(4n; m_1[l], m_2[r], m_3) \simeq D(4n; -m_1[l + 2], m_2[r], m_1 + m_3)$.

PROOF. By Theorem 3.7, one can check directly that the four diagrams are all alternating Heegaard diagrams. The first four homeomorphisms can be proved similarly to the proof of Lemma 3.5. For the last homeomorphism we only need to prove the following:

$$D(4n; m_1[-2], m_2, m_3) \simeq D(4n; -m_1, m_2, m_1 + m_3).$$

This can be shown as in Figure 33. Here we only give the left part of the surface. The notation x (or y) means that there are x (or y) parallel arcs and here $x = m_1$.

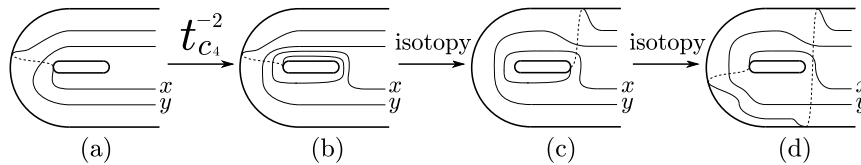


FIGURE 33. Dehn twist and isotopy.

Figure 33 (a) shows the left part of the diagram $D(4n; m_1, m_2, m_3)$. Applying the Dehn twist $t_{c_4}^{-2}$ on it, we get Figure 33 (b), the left part of $D(4n; m_1[-2], m_2, m_3)$.

This is isotopic to $D(4n; -m_1, m_2, m_1 + m_3)$, via two isotopies as in Figures 33 (c) and (d). \square

LEMMA 5.6. *The Dehn twist (half twist), π -rotation and reflection, as in Figure 14, map a weakly alternating Heegaard diagram to a weakly alternating Heegaard diagram.*

THEOREM 5.7. *A diagram is a weakly alternating Heegaard diagram if and only if it has the form $t_{c_1}^{m_4} t_{c_2}^{m_5} (D(4n; m_1[l], m_2[r], m_3))$, $n > 0$, m_i ($1 \leq i \leq 5$), l, r are all integers and satisfy $(m_1^2 - 1)l = (m_2^2 - 1)r = 0$.*

PROOF. *The Only If Part.* Suppose $\{\alpha_1, \beta_1, \gamma_1\} \cup \{\alpha_2, \beta_2, \gamma_2\}$ is a weakly alternating Heegaard diagram on a splitting surface S . We can assume $\{\alpha_2, \beta_2, \gamma_2\}$ to be standard as before and the curves $\{\alpha_1, \beta_1, \gamma_1\}$ to have colors red, green and black.

Cutting S along $\{\alpha_2, \beta_2, \gamma_2\}$, we get S_l and S_r . Since γ_1 intersects $\{\alpha_2, \beta_2, \gamma_2\}$ in the cyclic order $\alpha_2, \gamma_2, \beta_2, \gamma_2, \dots$, the black curve must be cut into arcs lying in S_l and S_r as in Figure 34.

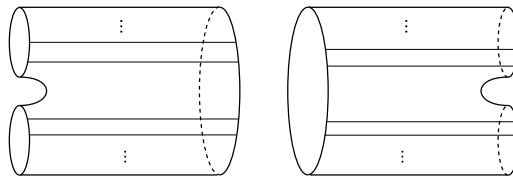


FIGURE 34. Black curves in S_l and S_r .

Since γ_2 intersects $\{\alpha_1, \beta_1, \gamma_1\}$ in the cyclic order $\alpha_1, \gamma_1, \beta_1, \gamma_1, \dots$, the number of intersection points with color red (green) must be even. Cutting S_l and S_r along the black arcs, since intersections of $\{\alpha_1, \beta_1, \gamma_1\}$ and $\{\alpha_2, \beta_2, \gamma_2\}$ are minimal (see Remark 5.2), each rectangle piece can contain only one red (green) arc.

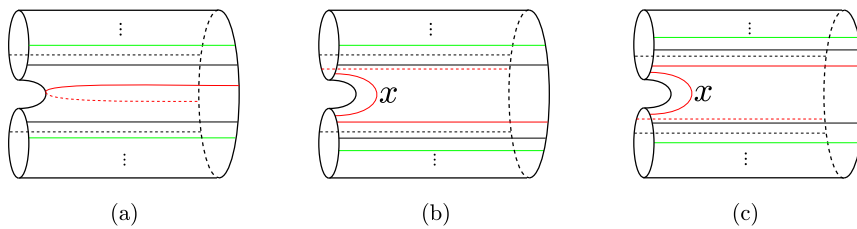


FIGURE 35. Three possibilities of colored arcs in S_l .

If the number of colored arcs in the saddle piece is not 2, then modulo the Dehn twist along α_2 (β_2) the pasting way at α_2 (β_2) is unique. Moreover, in any case all arcs in the saddle piece will have the same color. We recolor the

red (green) curves if it is needed, then S_l should be as in Figure 35. Here the notation x means there are x parallel arcs. The situation of S_r will be similar.

The original diagram can be obtained from S_l and S_r by pasting the cuts. Hence $t_{c_5}^{-r} t_{c_4}^{-l} t_{c_2}^{-m_5} t_{c_1}^{-m_4} (\{\alpha_1, \beta_1, \gamma_1\}) \cup \{\alpha_2, \beta_2, \gamma_2\}$ will become an alternating Heegaard diagram $D(4n; m_1, m_2, m_3)$, if we choose suitable m_4, m_5, l and r . When the number of colored arcs in the saddle piece of S_l or S_r is not 2, l or r is not 0 and correspondingly m_1 or m_2 must be ± 1 . Since $t_{c_1}^{m_4} t_{c_2}^{m_5}$ preserves the curves $\{\alpha_2, \beta_2, \gamma_2\}$, we know that $\{\alpha_1, \beta_1, \gamma_1\} \cup \{\alpha_2, \beta_2, \gamma_2\}$ has the form as in the theorem.

The If Part. By the definition of $D(4n; m_1[l], m_2[r], m_3)$, $D(4n; m_1[0], m_2[0], m_3)$ is always an alternating Heegaard diagram.

Let it be $\{\alpha_1, \beta_1, \gamma_1\} \cup \{\alpha_2, \beta_2, \gamma_2\}$. If m_1 or m_2 is ± 1 , then we can apply the Dehn twist $t_{c_4}^l$ or $t_{c_5}^r$ on $\{\alpha_1, \beta_1, \gamma_1\}$ to get weakly alternating Heegaard diagrams. Hence, by Lemma 5.6, the diagrams given in the theorem are all weakly alternating Heegaard diagrams. \square

6. Manifolds with weakly alternating Heegaard splittings

DEFINITION 6.1. Define $M_i(n; k_1[l], k_2[r], k_3)$ to be the 3-manifold which has a Heegaard diagram $D(4n; m_1[l], m_2[r], m_3)$ with $(m_1, m_2, m_3) = \eta_i + 4(k_1, k_2, k_3)$, $i = 1, 2$. Here η_i is as in Definition 4.1. $n > 0$, k_i, l and r are integers and $(n, k_1 + k_2 + 2k_3) = 1$.

LEMMA 6.2. *If a 3-manifold M admits a weakly alternating Heegaard splitting but does not admit an alternating Heegaard splitting, then M must be homeomorphic to one of the following:*

- (a) $M_1(n; 0[l], k_2, k_3)$, here $0 \leq k_3 < n$, $n \leq k_2 + 2k_3 < 2n$.
- (b) $M_1(n; 0[l], 1[r], k_3)$, here $0 \leq k_3 < n$.

PROOF. By Theorem 5.7 and modulo the Dehn twist $t_{c_1}^{m_4} t_{c_2}^{m_5}$, we only need to consider three classes of diagrams: $D(4n; \pm 1[l], m_2, m_3)$, $D(4n; m_1, \pm 1[r], m_3)$ and $D(4n; \pm 1[l], \pm 1[r], m_3)$.

Firstly we consider the first two classes. By Lemma 5.5, the 3-manifold which can be given by diagrams in these two classes can also be given by a diagram like $D(4n; 1[l], m_2, m_3)$. Then there are two subclasses: $D(4n; 1[l], -3 + 4k_2, 1 + 4k_3)$ and $D(4n; 1[l], -5 + 4k_2, 2 + 4k_3)$. But, by Lemma 5.5, we have

$$\begin{aligned}
 D(4n; 1[l], -3 + 4k_2, 1 + 4k_3) &\simeq D(4n; -1[l + 2], -3 + 4k_2, 2 + 4k_3) \\
 &\simeq D(4n; 1[-l - 2], -5 + 4(2 - k_2), 2 + 4(-1 - k_3)).
 \end{aligned}$$

Hence we only need to consider the diagrams $D(4n; 1[l], -3 + 4k_2, 1 + 4k_3)$ with $(n, k_2 + 2k_3) = 1$, which give us $M_1(n; 0[l], k_2, k_3)$. By Lemma 5.5 again, we can require $0 \leq k_3 < n$ and $n \leq k_2 + 2k_3 < 2n$.

Similarly for the third class we only need to consider $D(4n; 1[l], 1[r], 1 + 4k_3)$ with $(n, 1 + 2k_3) = 1$. These diagrams give us the manifolds $M_1(n; 0[l], 1[r], k_3)$, and we can require $0 \leq k_3 < n$. \square

PROPOSITION 6.3. $M_1(n; 0[l], k_2, k_3)$ ($M_1(n; 0[l], 1[r], k_3)$) as in Lemma 6.2 is a 2-fold branched cover of S^3 . The branched set is a three bridge link as in Figure 36 (a) (36 (b)).

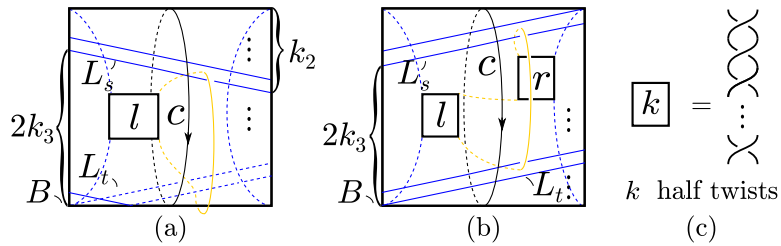


FIGURE 36. Branched set.

The front (back) blue arcs lying in the surface of the $n \times n$ square pillow have slope $-m/n$ (m/n), m is $k_2 + 2k_3 - n$ in Figure 36 (a) and is $1 + 2k_3 - n$ in Figure 36 (b). Walking from the point B to the right we get the arc L_t . Walking against the oriented circle c from L_t by $2k_3$ we get the arc L_s . Hence the position of the yellow arc can be determined. The k -box denotes two parallel arcs with k half twists. Over-crossings are from the lower left to the upper right if $k > 0$, and the upper left to the lower right if $k < 0$.

PROOF. We only prove the case of $M_1(n; 0[l], k_2, k_3)$. For $M_1(n; 0[l], 1[r], k_3)$ the proof will be similar.

Firstly consider the 2-fold branched cover from $M_1(n; 0[0], k_2, k_3)$ to S^3 . Figure 37 shows us the position of the Dehn twist curve c_4 in N_2 and its image c_4/τ in N_2/τ . Here τ is an involution.

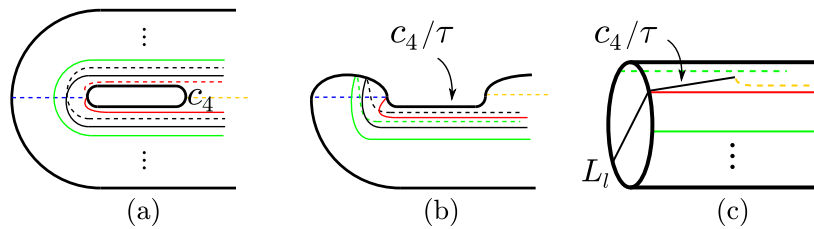


FIGURE 37. Position of c_4/τ .

Figure 37 (a) gives the left part of N_2 and Figure 37 (b) gives its quotient. This quotient can also be given by modulo the reflection along the line L_l in Figure 37 (c). One can compare Figure 37 (c) to Figure 22 (a).

By the proof of Proposition 4.3, the quotient $M_1(n; 0[0], k_2, k_3)/\tau$ has the branched set as in Figure 38 (a).

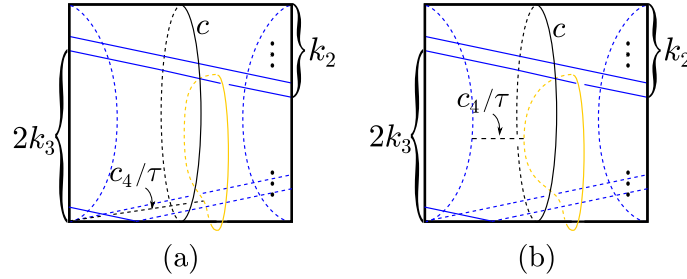


FIGURE 38. Push c_4/τ into the square pillow.

Notice that a Dehn twist along c_4 in S will induce a half twist around c_4/τ in S/τ . Hence for $M_1(n; 0[l], k_2, k_3)/\tau$, when we paste N_1/τ to N_2/τ , the gluing map will be different from the case of $M_1(n; 0[0], k_2, k_3)/\tau$ by l half twists around c_4/τ .

We can require these l half twists happen in a small neighbourhood of c_4/τ , and push c_4/τ and its neighbourhood into the square pillow as in Figure 38 (b). Then we will get the picture as in Figure 36 (a). □

PROPOSITION 6.4. *We have the following homeomorphisms:*

- (a) $M_1(n; 0[l], n + m, 0) \simeq L(n, m) \# L(l, 1), 0 \leq m < n.$
- (b) $M_1(n; 0[l], n - m, m) \simeq S^2(-1/2, 1/(l + 2), m/n), 0 < m < n.$
- (c) $M_1(n; 0[l], 1[r], 0) \simeq S^2(1/l, 1/s, 1/n), n > 0.$

PROOF. This proof is similar to the proof of Proposition 4.4 and the same argument as in Figure 24 will be used. For $M_1(n; 0[l], n + m, 0)$ the branched set is isotopic to the link as in Figure 39 (a). It is clear that the link is a connected sum. The 2-fold branched cover of this link is a connected sum of two Lens spaces.

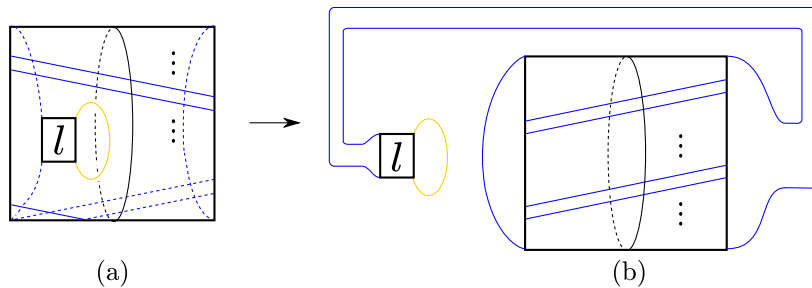


FIGURE 39. Connected sum of two bridge links.

For $M_1(n; 0[l], n - m, m)$ the branched set is isotopic to the link as in Figure 40 (a). Pushing the yellow arc into the square pillow, we will get Figure 40 (b).

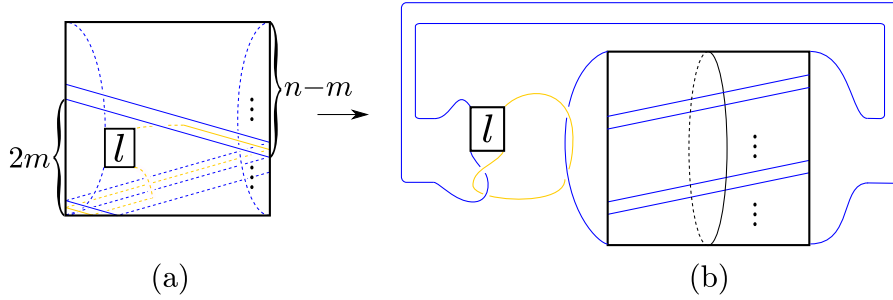


FIGURE 40. Montesinos link or connected sum.

When $l \neq -2$, it is a Montesinos link with three rational tangles having parameters $(1, l + 2)$, $(-1, 2)$ and (m, n) . When $l = -2$, this link is a connected sum of a two bridge link and a Hopf link. The corresponding 3-manifold is a Seifert fibred space or a connected sum. The manifold can be presented uniformly as $S^2(-1/2, 1/(l + 2), m/n)$.

For $M_1(n; 0[l], 1[r], 0)$ the branched set is isotopic to the link as in Figure 41 (a). When we take a half twist at the right-hand side of the square pillow, we will get Figure 41 (b), and this is isotopic to Figure 41 (c).

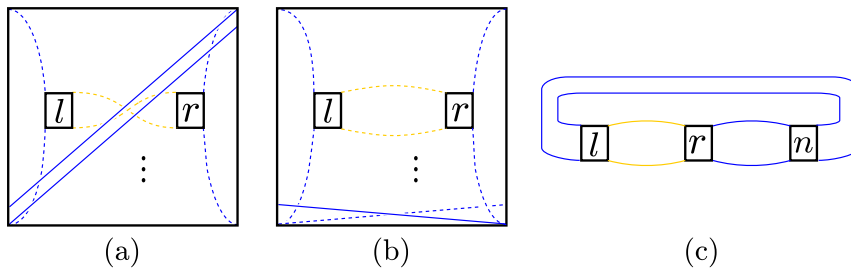


FIGURE 41. Pretzel link or connected sum.

Clearly when $l \neq 0$ and $r \neq 0$, it is a Montesinos link with three rational tangles having parameters $(1, l)$, $(1, r)$ and $(1, n)$. This is also a Pretzel link. When $l = 0$ or $r = 0$, it is a connected sum. The corresponding 3-manifold can be a Seifert fibred space, a connected sum of Lens spaces or a connected sum of a Lens space and $S^1 \times S^2$. The manifold can be presented uniformly as $S^2(1/l, 1/r, 1/n)$. \square

PROPOSITION 6.5. $M_2(5; 0[l], 4, 1) \simeq S^3_{l-2/1}(4_1) (\simeq M_1(5; 0[-l - 2], 3, 3))$.

PROOF. By the proofs of Propositions 4.3 and 6.3, it is not hard to see that the corresponding link of $M_2(n; 0[l], k_2, k_3)$ is as in Figure 42 (a). Hence the corresponding link of $M_2(5; 0[l], 4, 1)$ is as in Figure 42 (b), and it is isotopic to the link as in Figure 42 (c).

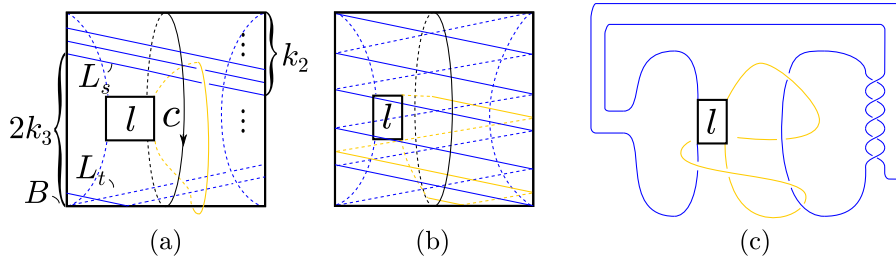


FIGURE 42. The quotient $M_2(5; 0[l], 4, 1)/\tau$.

On the boundary of the l -box we draw a green arc connecting two singular points and winding around the box $l/2$ rounds. It can be obtained from the trivial case by l half twists, see Figure 43 (a) for the case $l = 5$. Clearly the 2-fold branched cover of the box is a solid torus, and the 2-fold branched cover of this green arc is a green circle, which bounds a disk in the solid torus.

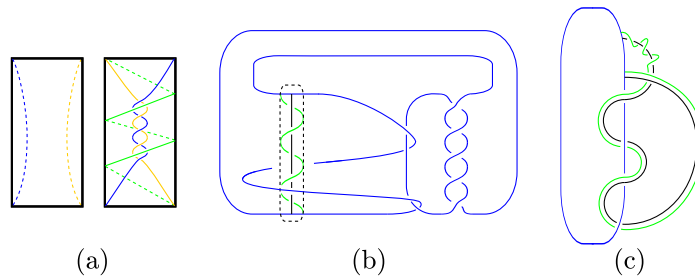


FIGURE 43. Surgery on $M_2(5; 0[l], 4, 1)/\tau$.

If we replace the l -box by a box containing two parallel horizontal singular arcs, then the singular set will be as in Figure 43 (b), which is a trivial knot. The new box can be thought as a regular neighbourhood of a regular arc, and the green arc winds around the regular arc $l/2$ rounds. We can move this picture to the position as in Figure 43 (c).

Then it is easy to see its 2-fold branched cover is S^3 and the 2-fold branched cover of the regular arc is a figure eight knot, as in Figure 44 (a).

Now the green circle winds around the regular circle $l - 2$ rounds. Removing the regular neighbourhood of the figure eight knot, since the circle which bounds a Seifert surface in the complement is parallel to the knot as in Figure 44 (b), we know that $M_2(5; 0[l], 4, 1)$ is the $l - 2$ surgery on the figure eight knot. \square

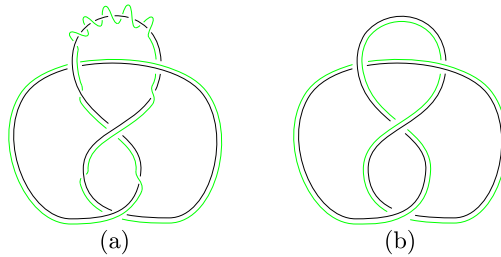


FIGURE 44. The figure eight knot.

REMARK 6.6. (a) The figure eight knot has exactly 10 exceptional slops, namely ∞ and $-4 \leq p/1 \leq 4$. Other $S^3_{p/1}(4_1)$ are all hyperbolic. The exceptional cases are listed below (see [8]).

- $S^3_\infty(4_1) \simeq S^3$.
- $S^3_{0/1}(4_1)$ is the T^2 -bundle over S^1 with monodromy $\begin{pmatrix} 1 & 1 \\ 1 & 2 \end{pmatrix}$. It admits the Sol geometry.
- $S^3_{\pm 1/1}(4_1) \simeq S^2(-1/2, 1/3, 1/7)$.
- $S^3_{\pm 2/1}(4_1) \simeq S^2(-1/2, 1/4, 1/5)$.
- $S^3_{\pm 3/1}(4_1) \simeq S^2(-2/3, 1/3, 1/4)$.
- $S^3_{\pm 4/1}(4_1)$ is a union of the trefoil knot complement and the twisted I -bundle over the Klein bottle. It contains an incompressible torus.

(b) One can also show that $M_2(n; 0[1], n - 3, 2) \simeq S^3_{n-2/1}(4_1)$ ($n \geq 5$) by a similar way. Compare it to Proposition 4.5.

REMARK 6.7. (a) $S^1 \times S^2 \# S^1 \times S^2$ is a genus two 3-manifold which has no weakly alternating Heegaard splitting. Otherwise $\pi_1 \cong \mathbb{Z} * \mathbb{Z}/H$ with H nontrivial. But $\mathbb{Z} * \mathbb{Z}/H \not\cong \mathbb{Z} * \mathbb{Z}$ because $\mathbb{Z} * \mathbb{Z}$ is Hopfian. Actually one can show that $S^1 \times S^2 \# S^1 \times S^2$ does not admit any automorphism f with $\Omega(f)$ consisting of Williams solenoids, whose defining neighbourhoods have genus $g \leq 2$. This is similar to the fact that $S^1 \times S^2$ does not admit any automorphism f with $\Omega(f)$ consisting of Smale solenoids.

(b) By Section 2.2 and Theorem 1.2, we see that globally there can be many non-homeomorphic Williams solenoids (handcuffs solenoids) in a given 3-manifold, as the non-wandering sets of non-conjugate automorphisms. The following question is natural, it has been studied in [6] in the case of Smale solenoids.

QUESTION. Given a 3-manifold M , what kind of Williams solenoids (with defining neighbourhoods having genus $g \leq 2$) can be globally realized as attractors in M ? How many of them?

(c) We have shown that half of Prism manifolds admit automorphisms f with $\Omega(f)$ consisting of two Williams solenoids. Hence it is natural to ask what about

the other half, namely $P(m, n)$ with $0 < n < m$? In the case of $S_{l/1}^3(4_1)$ one can ask what about other surgeries? Generally we can ask the following question.

QUESTION. Does a 3-manifold in the following classes (all having Heegaard genus two) admit an automorphism whose non-wandering set consists of Williams solenoids (with defining neighbourhood having genus $g \leq 2$)

- Seifert fibred spaces $S^2(a, b, c)$,
- surgeries on two bridge knots?

(d) The manifolds as in Lemmas 4.2 and 6.2 may give homeomorphic ones. But on the other hand, they can give many kinds of 3-manifolds. We wonder how to classify them and get more familiar genus two 3-manifolds admitting dynamics f such that $\Omega(f)$ consists of solenoid attractors and repellers.

REFERENCES

- [1] M. BOILEAU, S. MAILLOT AND J. PORTI, *Three-dimensional orbifolds and their geometric structures*, Panoramas et Synthèses 15. Société Mathématique de France, Paris 2003.
- [2] G. BURDE AND H. ZIESCHANG, *Knots*, de Gruyter Stud. Math. **5**, Walter de Gruyter, Berlin, New York, 1985.
- [3] B. JIANG AND Y. NI, S. WANG, *3-manifolds that admit knotted solenoids as attractors*, Trans. Amer. Math. Soc. **356** (2004), 4371–4382.
- [4] M. MONTESINOS, *Classical tessellations and three-manifolds*, Springer-Verlag, 1985.
- [5] J. MA AND B. YU, *Genus two Smale-Williams solenoid attractors in 3-manifolds*, J. Knot Theory Ramifications **20** (2011), 909–926.
- [6] ———, *The realization of Smale solenoid type attractors in 3-manifolds*, Topology Appl. **154** (2007), 3021–3031.
- [7] S. SMALE, *Differentiable dynamical systems*, Bull. Amer. Math. Soc. **73** (1967), 747–817.
- [8] W.P. THURSTON, *The geometry and topology of three-manifolds*, Lecture Notes, 1978.
- [9] R.F. WILLIAMS, *One-dimensional non-wandering sets*, Topology **6** (1967), 473–487.

Manuscript received December 3, 2014

accepted February 27, 2015

CHAO WANG
 School of Mathematical Sciences
 University of Science and Technology of China
 Hefei 230026, P.R. CHINA

E-mail address: chao_wang.1987@126.com

YIMU ZHANG
 Mathematics School
 Jilin University
 Changchun 130012, P.R. CHINA

E-mail address: zym534685421@126.com